Morphometric Analysis of an Ontogenetic Series of Dolphin Cranial Endocasts

Sierra J. Cleveland

Under the supervision of Dr. V. Louise Roth,
Department of Biology, Duke University

May 2019

_____
Research Supervisor

_____
Faculty Reader

_____
Director of Undergraduate Studies

Honors thesis submitted in partial fulfillment of the requirements for graduation with Distinction in Biology in Trinity College of Duke University

ABSTRACT

The earliest stages of life mark a critical period of brain growth and cranial expansion that has been thoroughly studied in many cognitively complex species but not in dolphins. Marine mammal protection policies restrict certain invasive avenues of research critical to understanding brain growth in other species, but previous studies have found success in using CT scans from deceased, stranded dolphins to understand brain morphology through endocranial data. Thus, this study aimed to utilize cranial endocasts as a proxy for brains. Using the 3D surface modeling program Avizo, I generated virtual cranial endocasts from CT scans of an ontogenetic series of dolphin skulls. The endocasts were then 3D printed and used to form a silicone mold in which the cerebrum and cerebellum were individually delineated, modeled with clay, and weighed. Specimen ages ranged from fetus to adult. Existing literature has shown that before birth, the growth of the dolphin cerebellum surpasses that of the cerebrum; it has been suggested that this is due to establishing basic motor functions controlled by the cerebellum in preparation for aquatic life. Thus, I predicted that after birth the growth rate of the cerebrum will be faster than that of the cerebellum as more cognitively complex behaviors such as social interaction develop. However, hindbrain data collected through these methods were imprecise and could not be used. Future research might have more success with different, more sturdy types of molds and mold-making materials. This method may best be applied to older specimens with more developed cerebella.

INTRODUCTION

Cetaceans possess oddly shaped and transversely broadened brains that are uniquely different from those of all other mammals (Buhl and Oelschläger 1988, Colbert *et al.* 2005). The evolution of the development of this peculiar brain morphology is particularly intriguing given the convergence of complex cognitive traits among other mammalian species that possess dissimilar brains (Marino 2002). During fetal development, all mammals share a common sequence of morphogenetic changes in their skulls and brains (Buhl and Oelschläger 1988). Deviations from this common sequence in the dimensions and structure are interpreted to be reflections of evolutionary adaptations pertinent to the unique environmental pressures of their ecological niches (Oelschläger 2008). Thus, the unusual shape and size of the cetacean brain have been interpreted to be a reflection of behavioral adaptations to the aquatic world (Marino 2002). Studying this relationship between anatomical development and behavioral ecology can provide insight into the evolutionary causes of this unique morphology. Moreover, there is a strikingly large gap in knowledge on this relationship in dolphin neonates, when behaviors start becoming more complex and different regions of the brain are activated. Few studies have examined the morphological ontogeny of the delphinid brain over the span of this early developmental period, through the fetal, neonatal (immediately before/after birth), and juvenile stages.

Research on fetal brain morphology has generally revealed that the volume of the cerebellum grows faster than that of the cerebrum during fetal development (Pirlot and Kamiya 1982). Though many mammals experience slightly more rapid cerebellar than cerebral growth prior to birth, few species possess as drastically different growth rates as dolphins. For example, throughout gestational development, fruit bat (*Artibeus jamaicensis*) cerebra increase sevenfold,

while cerebella increase eightfold; in dogs, they increase by a factor of 27.6 and 30.6, respectively (Pirlot and Kamiya 1982). In contrast, the striped dolphin (*Stenella coeruleoalba*) cerebrum increases tenfold before birth, while the cerebellum grows to 29.5 times its size (Pirlot and Kamiya 1982). Entering the constant instability of water is a challenge that land mammals do not have to overcome at birth (Pirlot and Kamiya 1982), which may explain the discrepancy in cerebellar and cerebral growth rates across these species. Delphinids are able to control their aquatic movement and respiration as soon as they are born (Mann and Smuts 1999, Reid *et al*. 1995), and the precision of these motor functions as well as equilibrium maintenance are largely controlled by the cerebellum (Morton and Bastian 2004, Wright *et al.* 2016) Thus, in fetal cetaceans, growth of the cerebellum surpasses growth of the cerebrum in preparation for the immediate and challenging physical demands of the aquatic world (Pirlot and Kamiya 1982, Parolisi *et al.* 2015).

Most studies of early delphinid development have examined the shape and size of the aggregate brain, but there is little information on how the cerebrum and cerebellum change throughout the entirety of the pre- and post-natal period. Pirlot and Kamiya 1982 studied a fetal ontogenetic series of *S. coeruleoalba* brains, that weighed 45.8g, 110g, and 517g. Their body lengths were 39 cm, 51 cm, and 95 cm, and the cerebellar fractions of the brain mass were 4.82%, 7.04% and 13.0%, respectively. Their range of specimens studied was limited to the prenatal period, so comparison with postnatal growth trends was not possible. Hence, this study does not provide sufficient information on how the transition from womb to water affects the morphological development of the brain as a juvenile. On the other hand, studies of juveniles have been less descriptive of the sizes of the individual regions of the brain and focused more on overall size and shape in relation to fully developed brains. Marino *et al.* 2004 reported that

neonatal *Tursiops* possess highly developed brains that weigh between 676g and 750g, which is on average 42.5% of adult brain weight, and by weaning age (18 months) their brains weigh over 80% of adult brain weight (Ridgway 1986). Thus, much of the brain growth occurs subsequent to birth.

Existing literature on the postnatal development of the delphinid brain has focused largely on the morphology of the entire brain, but there is a meager amount of literature on individual cerebrum and cerebellum development. Though the relative timing of the brain growth spurt varies widely among mammals (Dobbing and Sands 1979), perinatal studies in other species may provide insight into general growth patterns. Perinatal dolphins are born with a relatively large cerebellar fraction of the brain, 14.1%, and this fraction only grows to 18.2% once fully developed (Marino *et al.* 2001, Ridgway *et al.* 2016). In comparison, in newborn humans, the cerebellum only composes 5.62% of the total perinatal brain weight, though it grows to 13.3% of the total adult brain weight (Guihard-Costa and Larroche 1990, Svennerholm *et al.* 1997).

The growth disparity between these species might be attributed to the former giving birth to precocial young, and the latter, altricial. Cross-species comparisons, especially when examining newborn cerebellum size as a proportion of adult cerebellum size, offer tentative explanations for these differences in postnatal brain growth trends. However, it is essential to note that comparison of phylogenetically disparate animals requires consideration of many other factors such as body size, scaling trends, and phylogenetic context. Altricial dogs and humans are born with cerebella that are 5% and 18% of their adult cerebellum weight respectively, whereas precocial dolphins and fruit bats are born with cerebella that are 22% and 38% of their adult cerebellum weight respectively (Pirlot and Bernier 1974, Pirlot and Kamiya 1982,

Watson *et al.* 2006, Ridgway *et al.* 2016). Comparing these raw percentages does not account for the aforementioned factors but does present some disparities in brain growth between altricial and precocial species, in which the stage of behavioral development at birth is so different.

Nonetheless, precocial cetaceans are known to have relatively large cerebella (Ridgway *et al.* 2016). Given that a neonatal dolphin's cerebellum is 22% of adult size, that means that postnatally, it will need to increase in volume by a factor of 4.5x. And if its entire brain is 40% of adult size at birth, that means that postnatally the whole brain has to increase by a factor of 2.5. Therefore, if the cerebellum has to increase by a factor of 4.5, while the entire brain is increasing only by a factor of 2.5, then the cerebellum must grow proportionately faster, relative to the brain as a whole. However, these numbers are indicative of a lifetime trend from birth to adulthood. Individual growth rates of the cerebellum and cerebrum have not been directly studied during the early postnatal developmental period in delphinids where growth rates of different regions of the brain are constantly changing throughout physical and mental development. Brain development studies on other precocial species that focus solely on the neonatal period present contrasting evidence that could possibly be linked to behavioral development.

Domestic pigs (*Sus scrofa domesticus*), another precocial animal, experience a biphasic peak in cerebral growth rate approximately 25 days prior to birth, and 15 days after birth, the latter of which is accompanied by the rapid development of a competitive social hierarchy (Graves 1984, Pond *et al.* 2008). Piglets also experience a biphasic peak in cerebellar growth rate that is slightly offset from that of the cerebrum, approximately 5 days prior to birth, and 25 days after birth, around the same time as weaning. Although the cerebellum has also been associated with cognitive abilities and intelligence, the limbic system within the cerebrum has long been

regarded as the primary center for processing sensory input and controlling basic emotions, learning, memory, and innate drives such as dominance, sex, and parental care, (Paradiso 1997, Liem *et al.* 2001). While the velocity of cerebral and cerebellar growth in the perinatal pig brain has not been studied past the first 25 days post-parturition, the correlation between the early and rapid development of complex social behaviors and the earlier peaks in cerebral growth rate suggest that there may be a similar pattern in species with an equally swift and complex behavioral ontogenesis, such as delphinids.

In delphinids, early behavioral development is extremely rapid. Although young are precocial, in the first week after birth, infants are reliant on their mothers, independently swimming and breathing in constant synchrony; but by the second week, this synchrony begins to decline while infants practice other skills such as diving and floating (Mann and Smuts 1999, Lyamin *et al.* 2007). By the end of the second month, infants will have learned to socialize, engage in reciprocal chase games, use objects, practice foraging, tolerate longer separations from their mothers, and even produce adult-like echolocation pulses (Reiss 1988, Mann and Smuts 1999). The region of the brain responsible for these complex behaviors such as learning, memory, and communication is the cerebrum (Liem *et al.* 2001). Thus, the rapid development of these behaviors after birth suggest that the cerebrum may experience greater postnatal growth than the cerebellum, or if the cerebellum continues to grow faster, the difference in growth rates after birth narrows.

Research in early brain development in dolphins has been largely divided between only fetal or only neonatal specimens. Differences in study species in existing literature makes it difficult to compare the entire morphogenesis of the dolphin brain throughout the fetal, perinatal, and neonatal stages. Hence, this study attempts to address this gap in knowledge through a

morphometric analysis of an ontogenetic series of *Tursiops truncatus* fetal, neonatal, and juvenile specimens. I hypothesize that since the basic motor functions controlled by the cerebellum must be established in preparation for oceanic life before birth, and that, after birth more complex behaviors controlled by the cerebrum develop, such as social interaction and echolocation, the volumetric growth rate of the cerebellum will be seen to surpass that of the cerebrum before birth, and that after birth these growth patterns invert. To test my hypothesis, I generated 3D cranial endocasts from CT scans of dolphin skulls and conducted a morphological analysis on the axes of size increase, overall brain size, and cerebral and cerebellar growth. Increasingly strict marine mammal protection policies have limited research on the anatomy and physiology of dolphin brains to postmortem stranded specimens and use of noninvasive methods, such as MRI or CT scanning. Thus, this kind of digital data has become essential to our understanding of delphinid brain morphology.

METHODS

Several studies on cetacean brain growth have already utilized computed tomographic skull data to generate 3D reconstructions of the cranial vault (Colbert *et al.* 2005). However, because changes in the volume of the cranial endocast not only represent changes in brain volume itself, but also the ossification, thickening, and growth of the meningeal membrane surrounding the brain (Colbert *et al.* 2005), the direct translation of endocranial data to brain data is imperfect. Colbert *et al.* 2005 estimated the adult membrane to be 1.2mm thick, though it is unknown if this thickness changes during fetal and neonatal development. Thus, endocranial volume is expected to be approximately 3 to 4% bigger than the actual brain volume (Colbert *et al.* 2005). Additionally, cranial endocasts only yield morphological data on the external features

of the brain that were prominent enough to affect the skull; no internal brain features are revealed unless the skull was scanned with the brain intact, though ossified falx and tentorium may delineate the cerebral and cerebellar hemispheres in fully developed specimens. While specific and intricate regions of the brain may not be identifiable, the forebrain and hindbrain are clearly distinguishable in the cranial endocasts. Previous success with cranial endocast data suggests that this is a promising, noninvasive research method that could allow for a better understanding of the general morphological brain changes occurring in younger individuals that may be otherwise difficult to study. While remaining in compliance with marine mammal protection policies, this method utilizes already available and deceased specimens and leaves them intact for future research.

Specimens

Specimens include four postmortem skulls of an ontogenetic series of bottlenose dolphins (*Tursiops truncatus*) that stranded off the coast of North Carolina from 2015 to 2016. Specimens were retrieved and frozen heads were collected by the Marine Mammal Stranding Program under the direction of W.A. McLellan, D.A. Pabst, J.P. Kroeger, and T.F. Keenan-Bateman at the University of North Carolina, Wilmington. Heads were retained for scanning under a permit from the National Oceanographic and Atmospheric Administration obtained by R.A. Roston.

The adult specimen stranded in November 2016 in Caswell Beach, North Carolina (Field# WAM716). Total body length was 263 cm. He is classified as an adult, although the exact age is unknown. Male *Tursiops* reach their full body length of around 260 cm at around 15 years of age and can live for more than 40 years (Sergeant *et al.* 1973, Read *et al.* 1993, Reeves

et al. 2002). The male was observed to be freshly dead on the beach and necropsied the following day.

The juvenile specimen stranded in May 2015 on Topsail Island, North Carolina (Field# WAM 704). Total body length was 150.5 cm. Based on body length, age is estimated to be between 6 and 18 months (Sergeant *et al.* 1973, Marino *et al.* 2004). The male was dead upon inspection and the carcass was necropsied the following day.

The neonatal specimen stranded in May 2015 on Bald Head Island, North Carolina (Field# TFK 007). Sergeant *et al.* 1973 reported an average body length of 100 cm at birth for *T. truncatus* and total body length of this specimen was 107 cm. The female was found alive and euthanized on-site. The carcass was frozen for later examination.

The fetal specimen (Field# WAM 712F) was extracted from a pregnant female (Field# WAM 712) who had stranded in June 2016 on Oak Island, North Carolina. Total body length of the mother was 237.5 cm, and total body length of the male fetus was 59.5 cm. Frontal-occipital skull diameter was measured in Avizo. Based on a skull diameter of 5.7 cm, age is estimated to be 6 months post-conception (26 weeks prior to parturition) (Williamson *et al.* 1990).

Computed Tomography Scanning

All CT images were provided by R. A. Roston. S. Robinson, RVT, Diagnostic Imaging Supervisor at NC State Veterinary Hospital, Diagnostic Imaging Department, conducted CT scans of whole frozen heads from WAM716, WAM704, TFK007, and WAM712F using a Siemens Somatom Sensation 16 (Siemens Medical Solution, Malvern, PA) at NC State University, Raleigh, NC. Voxel size for WAM716 was 0.982031 x 0. 982031 x 0.6 mm. Voxel

size for WAM704 was 0.386719 x 0.386719 x 0.4 mm. Voxel size for TFK007 was 0.367188 x 0.367188 x 0.4 mm. Voxel size for WAM712F was 0.212891 x 0.212891 x 0.4 mm.

Three-Dimensional Reconstruction

3D reconstructions of cranial endocasts from CT scans of *T. truncatus* skulls were generated using the software program Amira-Avizo (Thermo Fisher Scientific) at Duke University. Segmentation of these scans utilized a Huion Graphics Drawing Tablet H420 (Shenzhen Huion Animation Technology, Shenzhen, China) to process 3,041 CT images in total (WAM712F: 476, TFK007: 778, WAM704: 951, WAM716: 836) in the sagittal, coronal, and transverse planes. Segmentation was executed in the plane in which the skull was most easily delineated (unique for each specimen/different parts of the brain), and the other planes were used to make corrections. I initially processed every fifth slice manually and used interpolation between them to minimize human error, but many additional slices required manual segmentation to reduce errors introduced by the automated processing.

Regions of error include spaces where bone was absent (e.g. sutures and foramina), requiring manual segmentation. These regions include the frontal bone, the ear bones, and the foramen magnum. However, after these gaps were filled, the remaining space was filled with the "magic wand" tool. The histogram was adjusted to select bone and create a unique material separate from the endocast. The histogram was then readjusted and the interior of the endocast was selected using the setting "same material only." This strategy minimized human error by allowing the computer to automatically generate more precise boundaries where bone was present. Other sources of error may be due to post-mortem handling. Because the fetal specimen was frozen and dissected before CT scanning, there is an apparent and shallow oval

indentation of a large area located on the right hemisphere where the parietal bone was pushed in.

Volume Estimates from 3D-Printed Endocasts

Total endocranial volume data were calculated directly from the endocasts in Amira-Avizo. To estimate the volume of the hindbrain, 3D prints were generated from each virtual endocast (except the adult due to printing issues and time constraints) and used to create a silicone mold, which was then filled with clay to measure the volume of the hindbrain compartment. The total volume of the mold was also measured in order to determine the accuracy of this method.

To create the silicone mold, a thin layer of pure Silicone 1 was poured over the endocasts and left to cure for 24 hours. Once dry, the molds were cut in half along the dorsal sagittal sinus and removed from the 3D prints. As a control, the fetal endocast was 3D printed to scale, its silicone mold filled completely with clay, and weighed. Volumetric data collected from this (conversion method listed below) was compared to the total endocranial volume calculated by Avizo and assessed for accuracy. The total volumes for the neonatal and juvenile molds were also recorded. Crayola modeling clay was then used to model the hindbrain within each half of the silicone mold. Previously published sagittal views of a *Tursiops truncatus* brain were used to delineate boundaries between the cerebellum and cerebrum (Marino *et al.* 2001a). Prior to modeling, the initial volume and weight of the clay were used to calculate the density (ρ=1.759). To calculate the initial volume of the clay, the height, length, and width of the modeling clay, prepackaged in the shape of a solid rectangular block, was measured and multiplied. After modeling, the weight of the hindbrain was divided by the density of the clay to calculate the

volume. This process was repeated three times to generate the average hindbrain volume, and then the standard deviation and coefficients of variation of each specimen's hindbrain volume was calculated and graphed in Excel. Additionally, the shallow indentation (see Results and Fig. 1a for full description) on the fetal endocast was covered in clay, weighed, and converted to volume to approximate the volume of tissue displaced or compressed in that region. This process was repeated three times; the data was then averaged, and the standard deviation was calculated.

RESULTS AND INTERPRETATION

Description of the Cranial Endocasts

Terminology used here is in accordance with the anatomical nomenclature used in Colbert *et al.* 2005.

All of the endocasts exhibit morphology consistent with that of dolphin brains: globular, transversely broadened, and foreshortened (Buhl and Oelschläger 1988, Colbert *et al.* 2005). Fine detail of external brain features such as sulci and gyri are obscured by the presence of blood sinuses and the meningeal membrane (Colbert *et al.* 2005). However, more general and discernible brain features are apparent in this ontogenetic series, such as the boundary between forebrain and hindbrain, the dorsal sagittal sinus, sutures, and the pyramidal tract impression.

Development of the hindbrain is evident; the fetal hindbrain is small (Fig. 1a), while the adult hindbrain (Fig. 1s) is large and prominent. Comparison of the neonatal and juvenile specimens reveal the extension of the hindbrain in the postero-ventral direction during development. Forebrain development can also be seen to a less obvious extent. The forebrain of the fetus is relatively round, but as development progresses, the forebrain begins to extend rostrally.

The dorsal sagittal sinus appears to be deepening throughout the dorsal and caudal series. However, in these regions of the endocast, it is difficult to distinguish between changes in brain morphology and development and changes in quantities of fluid in the blood sinuses. Alternatively, it may be that the left and right cerebral hemispheres are growing dorsally. Nonetheless, differences between each specimen are apparent. In the fetal endocast, the dorsal sagittal sinus is only slightly visible at the medial base of the cerebrum superior to the foramen magnum (Fig. 1e). In the neonatal endocast, it is more pronounced (Fig. 1k) but less so than in the juvenile endocast. The juvenile dorsal sagittal sinus is well-developed (Fig. 1q), and the adult is completely developed (Fig. 1w).

Sutures are visible on the cerebra of the fetal, neonatal, and juvenile endocasts. The coronal suture, where the frontal and interparietal bones have not yet completely fused, is prominently visible in the fetus (Fig. 1d and e), not as much in the neonate (Fig. 1j and k), and just slightly visible in the juvenile (Fig. 1p). In the neonate, sutures delineating the boundaries of the parietal and frontal/occipital bones (Fig. 1g, h, i, j, k) are more visible than in the fetus; they are less visible, but still present in the juvenile (Fig. 1m, n, o, p, q). It is important to note that on the right lateral side of the fetus (Fig. 1a), the ridges bordering a large oval compressed region are due to postmortem mishandling of the parietal bone. The right cerebral lobe appears slightly lopsided due to this (Fig. 1c).

Another feature to note is the pyramidal tract impression, which is visible in all but the fetal specimens. It is located on the ventral surface of the cerebellum medial to the temporal bones (Fig. 1l, r, x).

The striations seen on the inferior aspect of the fetal endocast, located at the foramen magnum (Fig. 1c) and the frontal bone (Fig. 1d), are artifacts of manual segmentation. The other

endocasts also possess similar striations (Fig. 1g, h, k, o). The gaps where the tympanic and squamous temporal bones reside also produced artifacts of manual segmentation, manifested as two protruding spikes on the ventral side of the cerebellum, distally located from one another, best visible in the right and left lateral views of each endocast. In the perinatal endocast, these protrusions extend from the cerebellum. Additionally, on the neonatal endocast, there is a small, deep, circular penetration inferior to the striations that was also a result of manual segmentation of the frontal bone (Fig 1j).

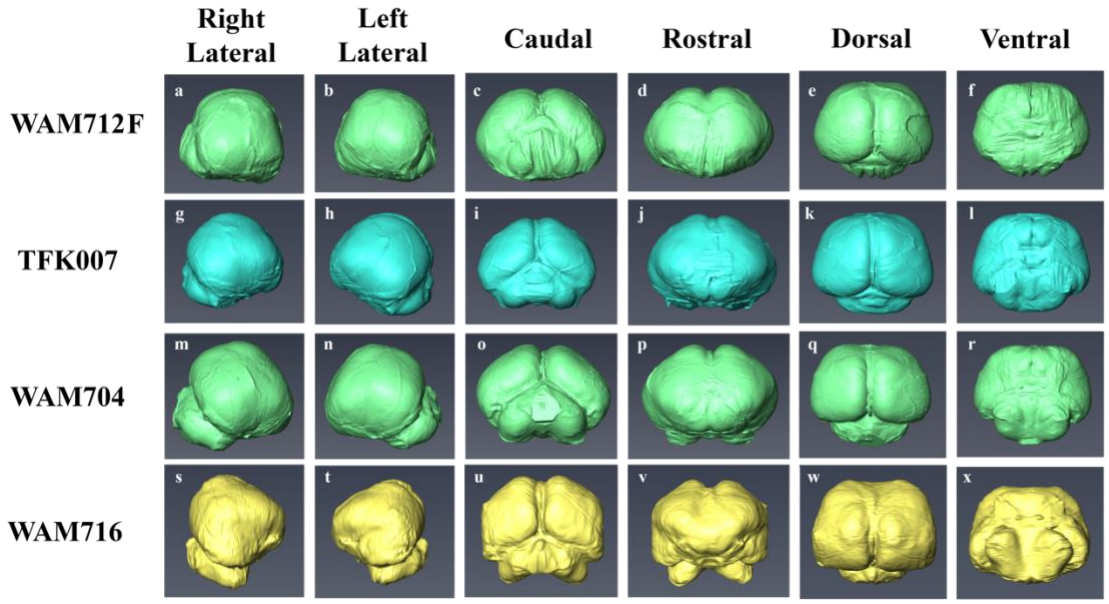

Figure 1a-x. Right/left lateral, caudal, rostral, dorsal, and ventral views of each cranial endocast. Endocasts were generated in Avizo from CT scans of postmortem bottlenose dolphins. Regions requiring manual segmentation include the foramen magnum, frontal bone, and ear bones. Before scanning, the right parietal bone of the WAM712F skull had been pushed in, compressing the endocast; the ridges surrounding this large oval region are visible in the right lateral view (Fig. 1a).

Total Endocranial Volume

Total volume estimates for each virtual cranial endocast are presented in Table 1. Endocranial volume and body length were logarithmically transformed and plotted using Excel

(Fig. 2). Isometry between length (cm) and volume (cm^3) is determined by an allometric coefficient of 3. The allometric coefficient of the line in Figure 2 is 1.161, thus the two variables exhibit a negative allometric relationship, i.e. endocranial volume change is slower than body length change. The volume of the compressed region in the fetal endocast was estimated to be 1.37 cm^3 (St. dev. = 0.13, n = 3), which is 0.7% of the total endocast, too small to be discriminated on Figure 2 below.

	Age Class	**Total Body Length (cm)**	**Total Endocranial Volume (cm^3)**
WAM 712F	Fetus (6 mo)	59.5	161
TFK 007	Neonate (at birth)	107	810
WAM 704	Juvenile (1 yr)	150	1109
WAM 716	Adult (15+ yrs)	263	1845

Table 1. Total volume of each virtual endocast. Specimen ages were estimated from frontal-occipital skull diameter measured in Avizo (WAM712F), or total body length (TFK007, WAM704, WAM716). Data were collected from virtual endocasts generated and analyzed in Avizo.

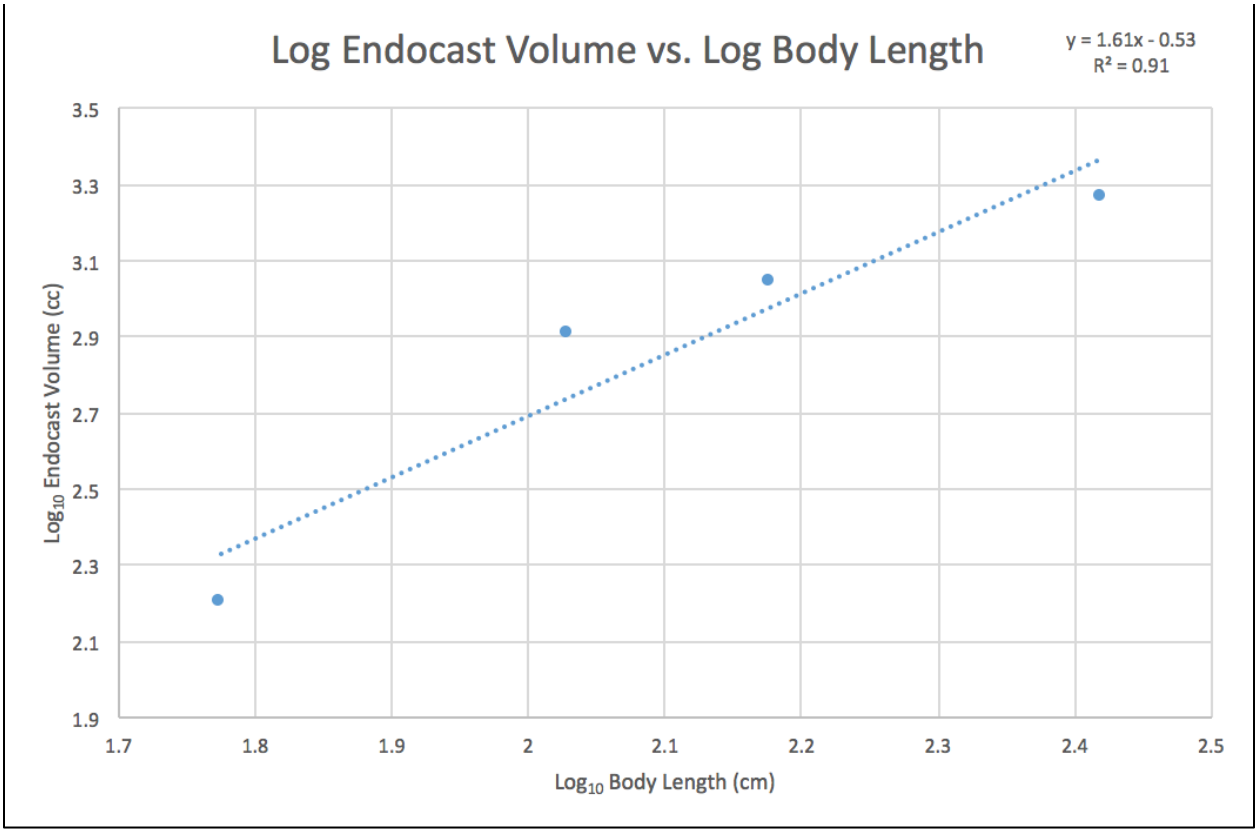

Figure 2. Allometric relationship between endocranial volume and body length. Logarithmically transformed data were plotted and fit to a linear trend line in Excel.

3D Printed Volume Estimates

The dimensions of the printed fetal endocast were 79.38 mm (left-right lateral), 64.20 mm (dorsal-ventral), 66.36 mm (rostral-caudal). The dimensions of the printed neonatal endocast were 103.55 mm, 80.98 mm, 84.31mm, and the dimensions of the printed juvenile endocast were 111.37 mm, 88.41 mm and 91.11 mm respectively.

The average of the three replicates for the fetal, neonatal, and juvenile specimens are listed in Table 2, accompanied by their standard deviations and coefficients of variation. Additionally, the total volume of each silicone mold is listed. The fetal endocast was printed to scale as a control and the total volume yielded 10% error. The coefficients of variation decrease

with age; there is much higher variance when the cerebellum is small. Figure 3 depicts the log of each hindbrain volume, with error bars, as a function of the log of the total volume of the mold. In the fetal specimen, the hindbrain comprised between 5.5% and 14.7% of the total endocranial volume, with an average of 10.1%. In the neonate, the hindbrain percentage was between 13.2% and 17.7%, with an average of 15.4%. In the juvenile, it was between 19.6% and 22.3%, with an average of 20.9%.

The high percent error of the control and the high coefficients of variation of the fetal hindbrain volume estimates provide evidence that this method is imprecise. Additionally, the range of volume estimates of the fetal cerebellum were much larger than published values in the literature. Pirlot and Kamiya 1982 reported a cerebellar fraction of just 7% of the total brain volume for a 51-cm *S. coeruleoalba* fetus, and 13% for a 95-cm fetus (considered to be close to birth). Despite this, the neonatal and juvenile specimens in this study yielded ranges of cerebellar volumes closer to published data. Newborn *Tursiops* cerebella account for 14% of the total brain volume and grow to 18.2% once fully mature (Marino *et al.* 2001b, Ridgway *et al.* 2016).

	Total Volume (cm^3)	**Average Hindbrain Volume (cm^3)**	**Standard Deviation**	**Coefficient of Variation**
WAM 712F	177.2	17.9	8.2	0.46
TFK 007	325.2	50.2	7.3	0.15
WAM 704	398.8	83.6	5.5	0.07

Table 2. Total volume of each silicone mold; average raw hindbrain volume estimates including the standard deviation and coefficients of variation. Total volume and hindbrain volume were measured by modeling clay in the silicone mold in accordance with previously published MRI images of *Tursiops* brains. Standard deviation and coefficients of variation were calculated in Excel.

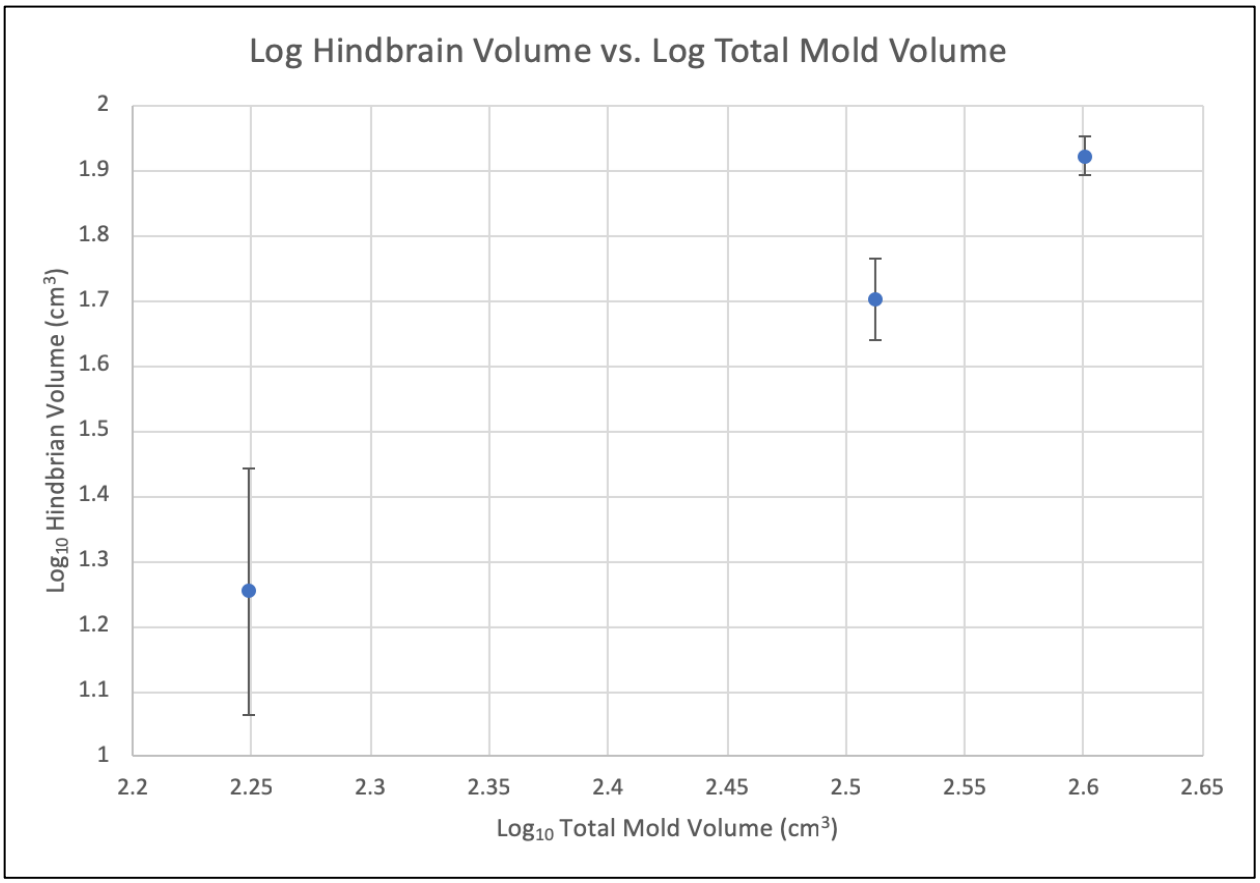

Figure 3. Log of average hindbrain volume with error bars. Data were logarithmically transformed and plotted in Excel.

DISCUSSION

The general shape of all of the endocasts is consistent with descriptions of *Tursiops* brains in the literature as well as other published 3D reconstructions (Marino *et al.* 2001b, Montie *et al.* 2007). Cetacean brains are foreshortened and transversely elongated (Buhl and Oelshläger 1988, Colbert *et al.* 2005); the endocasts exhibit these features. The rate of change in endocranial volume between each specimen is slower than that of body length, as expected; all vertebrate brains grow negatively allometrically with body size (Roth and Dicke 2005). As represented by the individual data points on Fig. 2, the change in the brain:body relationship between fetal and

neonatal stages compared to the changes postnatally suggest that brain growth relative to body growth decelerates after birth. However, additional samples are needed to verify that the apparent postnatal deceleration is robust. The displaced volume of the compressed region on the fetal endocast did not make a significant difference in any of these trends.

The computer-generated endocranial volumes for each specimen are in accordance with brain volumes of dolphins in the same age class. The 6-month old fetal *Tursiops* endocast had a volume of 161 cm^3. Marino *et al.* 2001b reported a brain volume of 195 cm^3 for a fetal *Delphinus delphis* 8-9 months post-conception. The 107 cm neonatal specimen had an endocranial volume of 810 cm^3, compared to a brain volume of 821 cm^3 for a 137 cm newborn *Lagenorhynchus acutus*, published by Montie *et al.* 2008. The same study reported a brain volume of 1019 cm^3 for a 156 cm specimen of that species, while this study found an endocranial volume of 1109 cm^3 for the 150 cm specimen.

Ridgway and Brownson 1984 found that the average adult *Tursiops* brain weight is 1587.5 ± 173.2 g; several other studies have supported this range (Roth and Dicke 2005, Ridgway *et al.* 2016, 2017). It is possible to compare brain weight to brain volume by dividing the weight by the average specific gravity of cetacean brains, 1.04 (Ridgway *et al.* 2017). The adult male specimen in this study had an endocranial volume of 1845 cm^3, which converts to an estimated weight of 1,918g and is slightly larger than the value given above. However, it is slightly smaller than Colbert *et al.* 2005's findings of an adult male *Tursiops gilli* (which Colbert. *et al* 2005 considered synonymous with *T. truncatus*) with an endocranial volume of 2048 cm^3 (weight = 2,130g). Due to the lack of endocranial studies, it is unknown if 11% variation in endocranial volume is common, but it could be explained by age or other individual differences. Furthermore, 3-4% of the endocranial volume can be attributed to the meningeal membrane

(Colbert *et al.* 2005). The volumetric data reported in Table 1 have not deducted this, and thus might account for some of the differences between the endocranial data collected from this study and previously reported brain weights.

The clay-modeling method was highly imprecise and subjective. The control (fetus) yielded a 10% error in total volume. This could be explained by the elasticity of shell silicone molds; they are flimsy and easily stretched. A sturdier type of silicone mold such as a two-part block mold would be more accurate, but a different, more rigid modeling material such as gypsum plasters could be used. Similarly, hollow shells of each endocast cut in half in the sagittal plane could be 3D printed and used to model the hindbrain with clay.

Because the silicone molds were cut in the sagittal plane, the surface area for each half of the fetal cerebellum was small and it was difficult to delineate the boundaries of the hindbrain. However, as the hindbrain grew, it became easier to model the hindbrain. This may explain why the fetal hindbrain volume estimates yielded such a high coefficient of variation compared to that of the other specimens. Future research modeling clay in molds will likely be more successful with a blanket mold in which the rostral part of the brain is fixed to a base and not covered by silicone, while silicone is poured over the hindbrain and left to cure. Through this method, the boundaries of the surface area of the hindbrain would be more easily delineated. Furthermore, because the coefficients of variation decrease with age, this methodology is best applied to older specimens with more developed cerebella.

Though these methods were imprecise, the results of the silicone-mold experiment offer preliminary insight into the growth of the cerebellum after birth. The increasing percentages presented on p.16 suggest that the cerebellar proportion of the brain increases through ontogeny, especially after birth, which is contrary to the original hypothesis. Although more data are

needed to support this apparent trend, these findings suggest that there may be a more complex relationship between volumes of brain structures and behavioral changes than originally predicted.

ACKNOWLEDGEMENTS

I would like to thank Dr. V. Louise Roth for her guidance and support in this project. I would also like to thank Rachel A. Roston for providing the CT images of the specimens (retained under the NOAA permit in her name) and the modeling clay, as well as her hands-on mentorship in the design of my research.

This would not have been possible without the Marine Mammal Stranding Program under the direction of W.A. McLellan, D.A. Pabst, J.P. Kroeger, and T.F. Keenan-Bateman at the University of North Carolina, Wilmington, who provided the specimens. CT imaging was carried out by S. Robinson of the Diagnostic Imaging Dept. at NC State University Veterinary Hospital.

Additional thanks to the Donohue lab for allowing me to use the scale in their laboratory, as well as the 3D printing team at the Innovation Co-Lab for their assistance in printing.

REFERENCES

Buhl, E. H., & Oelschläger, H. A. (1988). Morphogenesis of the brain in the harbour porpoise. *Journal of Comparative Neurology, 277*(1), 109-125. doi:10.1002/cne.902770108

Colbert, M. W., Racicot, R., & Rowe, T. (2005). Anatomy of the Cranial Endocast of the Bottlenose Dolphin, *Tursiops truncatus*, Based on HRXCT. *Journal of Mammalian Evolution,12*(1-2), 195-207. doi:10.1007/s10914-005-4861-0

Dobbing, J., & Sands, J. (1979). Comparative aspects of the brain growth spurt. *Early Human Development,3*(1), 79-83. doi:10.1016/0378-3782(79)90022-7

Graves, H. B. (1984). Behavior and Ecology of Wild and Feral Swine (*Sus scrofa*). *Journal of Animal Science,58*(2), 482-492. doi:10.2527/jas1984.582482x

Guihard-Costa, A., & Larroche, J. (1990). Differential growth between the fetal brain and its infratentorial part. *Early Human Development,23*(1), 27-40. doi:10.1016/0378-3782(90)90126-4

Liem, K. F., Bemis, W. E., Walker, W. F., Jr., & Grande, L. (2001). The Nervous System II: The Brain. In *Functional anatomy of the vertebrates: An evolutionary perspective* (3rd ed., pp. 474-503). Belmont, CA: Brooks / Cole Cengage Learning.

Lyamin, O., Pryaslova, J., Kosenko, P., & Siegel, J. (2007). Behavioral aspects of sleep in bottlenose dolphin mothers and their calves. *Physiology & Behavior,92*(4), 725-733. doi:10.1016/j.physbeh.2007.05.064

Mann, J., & Smuts, B. (1999). Behavioral Development In Wild Bottlenose Dolphin Newborns (*Tursiops Sp*.). *Behaviour,136*(5), 529-566. doi:10.1163/156853999501469

Marino, L., Sudheimer, K., Murphy, T. L., Davis, K. K., Pabst, D. A., McLellan W. A., Rilling J. K., Johnson J.I. (2001a). Anatomy and three-dimensional reconstructions of the bottlenose dolphin (*Tursiops truncatus*) brain from Magnetic Resonance Images. *The Anatomical Record,264*, 397-414.

Marino, L., Murphy, T. L., Gozal, L., & Johnson, J. I. (2001b). Magnetic resonance imaging and three-dimensional reconstructions of the brain of a fetal common dolphin, *Delphinus delphis*. *Anatomy and Embryology,203*(5), 393-402. doi:10.1007/s004290100167

Marino, L. (2002). Convergence of Complex Cognitive Abilities in Cetaceans and Primates. *Brain, Behavior and Evolution,59*(1-2), 21-32. doi:10.1159/000063731

Marino, L., Sudheimer, K., Pabst, D. A., Mclellan, W. A., Arshad, S., Naini, G., & Johnson, J. I. (2004). Anatomical Description of an Infant Bottlenose Dolphin (*Tursiops truncatus*) Brain from Magnetic Resonance Images. *Aquatic Mammals,30*(2), 315-326. doi:10.1578/am.30.2.2004.315

Montie, E. W., Schneider, G. E., Ketten, D. R., Marino, L., Touhey, K. E., & Hahn, M. E. (2008). Neuroanatomy of the Subadult and Fetal Brain of the Atlantic White-sided Dolphin (*Lagenorhynchus acutus*) from in Situ Magnetic Resonance Images. *The Anatomical Record: Advances in Integrative Anatomy and Evolutionary Biology,290*(12), 1459-1479. doi:10.1002/ar.20612

Morton, S. M., & Bastian, A. J. (2004). Cerebellar Control of Balance and Locomotion. *The Neuroscientist,10*(3), 247-259. doi:10.1177/1073858404263517

Oelschläger, H. H. (2008). The dolphin brain—A challenge for synthetic neurobiology. *Brain Research Bulletin,75*(2-4), 450-459. doi:10.1016/j.brainresbull.2007.10.051

Paradiso, S., Andreasen, N.C., O'Leary, D.S., Arndt, S., Robinson, R.G. (1997). Cerebellar size and cognition: correlations with IQ, verbal memory and motor dexterity. *Neuropsychiatry, Neuropsychology, and Behavioral Neurology,* 10(1) 1-8. PMID: 9118192.

Parolisi, R., Peruffo, A., Messina, S., Panin, M., Montelli, S., Giurisato, M., . . . Bonfanti, L. (2015). Forebrain neuroanatomy of the neonatal and juvenile dolphin (*T. truncatus and S. coeruloalba*). *Frontiers in Neuroanatomy,9*. doi:10.3389/fnana.2015.00140

Pirlot, P., & Bernier, R. (1974). Embryonic brain-growth in a fruit bat. *Anatomy and Embryology,146*(2), 193-208. doi:10.1007/bf00315595

Pirlot, P., & Kamiya, T. (1982). Embryonic brain-growth in a dolphin. *Anatomy and Embryology,164*(1), 43-50. doi:10.1007/bf00301877

Pond, W. G., Boleman, S. L., Fiorotto, M. L., Ho, H., Knabe, D. A., Mersmann, H. J., . . . Su, D. R. (2008). Perinatal Ontogeny of Brain Growth in the Domestic Pig. *Proceedings of the Society for Experimental Biology and Medicine,223*(1), 102-108. doi:10.1111/j.1525-1373.2000.22314.x

Read, A. J., Wells, R. S., Hohn, A. A., & Scott, M. D. (1993). Patterns of growth in wild bottlenose dolphins, *Tursiops truncatus*. *Journal of Zoology, London,231,* 107-123.

Reeves, R., Stewart, B., Clapham, P., & Powell, J. (2002). *National Audubon Society Guide to Marine Mammals of the World* (pp. 362-365). NY: A. A. Knopf. ISBN 978-0-375-41141-0.

Reid, K., Mann, J., Weiner, J. R., & Hecker, N. (1995). Infant development in two aquarium bottlenose dolphins. *Zoo Biology,14*(2), 135-147. doi:10.1002/zoo.1430140207

Reiss, D. (1988). Observations on the Development of Echolocation in Young Bottlenose Dolphins. *Animal Sonar,*121-127. doi:10.1007/978-1-4684-7493-0_14

Ridgway, S. H., & Brownson, R. H. (1984). Relative brain sizes and cortical surface areas in odontocetes. *Acta Zoologica Fennica,172,* 149-152.

Ridgway, S. H. (1986). Physiological Observations on Dolphin Brains. In *Dolphin Cognition and Behavior: A Comparative Approach* (pp. 31-59). Hillsdale, NJ: Lawrence Erlbaum Associates.

Ridgway, S. H., Carlin, K. P., Alstyne, K. R., Hanson, A. C., & Tarpley, R. J. (2016). Comparison of Dolphins Body and Brain Measurements with Four Other Groups of Cetaceans Reveals Great Diversity. *Brain, Behavior and Evolution,88*(3-4), 235-257. doi:10.1159/000454797

Ridgway, S. H., Carlin, K. P., & Alstyne, K. R. (2017). Delphinid brain development from neonate to adulthood with comparisons to other cetaceans and artiodactyls. *Marine Mammal Science,34*(2), 420-439. doi:10.1111/mms.12464

Roth, G., & Dicke, U. (2005). Evolution of the brain and intelligence. *Trends in Cognitive Sciences,9*(5), 250-257. doi:10.1016/j.tics.2005.03.005

Sergeant, D. E., Caldwell, D. K., & Caldwell, M. C. (1973). Age, Growth, and Maturity of Bottlenose Dolphin (*Tursiops truncatus*) from Northeast Florida. *Journal of the Fisheries Research Board of Canada,30*(7), 1009-1011. doi:10.1139/f73-165

Svennerholm, L., Boström, K., & Jungbjer, B. (1997). Changes in weight and compositions of major membrane components of human brain during the span of adult human life of Swedes. *Acta Neuropathologica,94*(4), 345-352. doi:10.1007/s004010050717

Watson, R. E., Desesso, J. M., Hurtt, M. E., & Cappon, G. D. (2006). Postnatal growth and morphological development of the brain: A species comparison. *Birth Defects Research Part B: Developmental and Reproductive Toxicology,77*(5), 471-484. doi:10.1002/bdrb.20090

Williamson, P., Gales, N. J., & Lister, S. (1990). Use of real-time B-mode ultrasound for pregnancy diagnosis and measurement of fetal growth rate in captive bottlenose dolphins (*Tursiops truncatus*). *Reproduction,88*(2), 543-548. doi:10.1530/jrf.0.0880543

Wright, M., Skaggs, W., & Nielsen, F. Å. (2016). The Cerebellum. *WikiJournal of Medicine,3*(1). doi:10.15347/wjm/2016.001